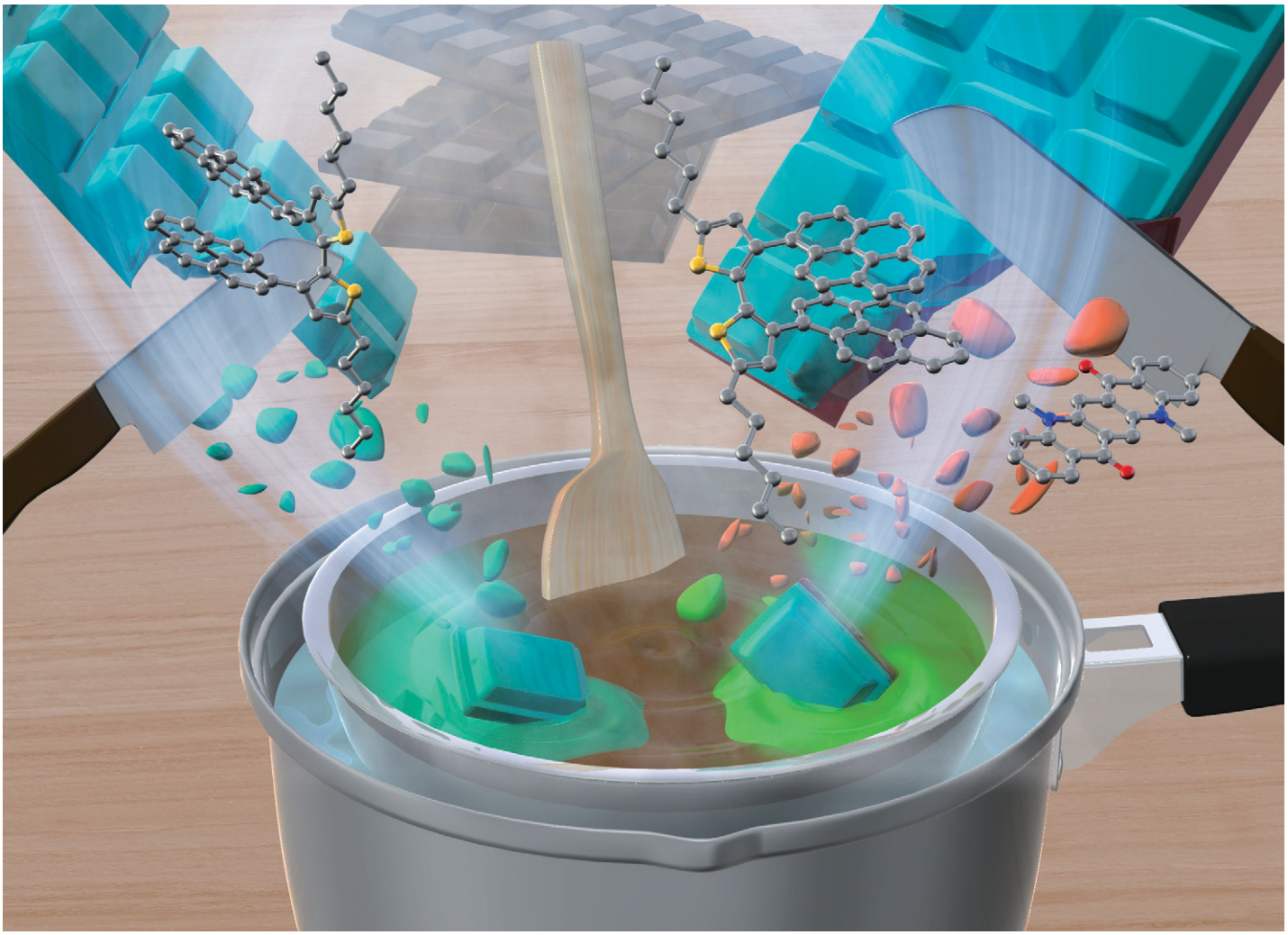

Showcasing research by Suguru Ito, Genki Katada, Tomohiro Taguchi, Izuru Kawamura, Takashi Ubukata, and Masatoshi Asami from Yokohama National University, Japan

Tricolor mechanochromic luminescence of an organic two-component dye: visualization of a crystalline state and two amorphous states

A two-component mixture of dipyrenylbithiophene and *N*,*N*′-dimethylquinacridone exhibited a tricolor mechanochromic luminescence (MCL), which should be attributed to the transition of dipyrenylbithiophene from a crystalline to two amorphous states. In contrast, dipyrenylbithiophene showed a poor MCL between two colors.

As featured in:

See Suguru Ito *et al.*, *CrystEngComm*, 2019, **21**, 53.

ROYAL SOCIETY OF CHEMISTRY | Celebrating IYPT 2019

rsc.li/crystengcomm

Registered charity number: 207890

CrystEngComm

PAPER

View Article Online
View Journal | View Issue

Cite this: *CrystEngComm*, 2019, **21**, 53

Tricolor mechanochromic luminescence of an organic two-component dye: visualization of a crystalline state and two amorphous states†

Suguru Ito, * Genki Katada, Tomohiro Taguchi, Izuru Kawamura, Takashi Ubukata and Masatoshi Asami

Solid-state emissive dyes with mechanochromic luminescence (MCL) properties change their emission colors upon exposure to mechanical stimuli. During the recent rapid advances in the area of MCL, considerable efforts have been focused on elucidating the MCL behavior of single-component dyes that can switch their solid-state emission between two colors. Herein, a novel strategy to achieve tricolor MCL is presented, which is based on mixing two organic dyes that exhibit poor MCL or no MCL properties, respectively. We propose that the tricolor MCL of the two-component dye should be attributed to the transition of the fraction with poor MCL properties from a crystalline to two amorphous states, specifically a perfectly amorphous and a proto-crystalline amorphous state. The present system should have advantages in terms of the availability of MCL dyes and the variety of potential combinations of two-component dyes. By making a use of the underlying design principle developed in this study, a wide variety of new MCL systems should be accessible, which should also accelerate the investigation of practical applications of MCL dyes.

Received 7th October 2018,
Accepted 19th November 2018

DOI: 10.1039/c8ce01698d

rsc.li/crystengcomm

Introduction

Mechanochromic luminescence (MCL) refers to a reversible shift of the solid-state emission maximum of a luminescent dye induced by the exposure to a mechanical stimulus (*e.g.* shearing, grinding, or pressure). Luminophores with MCL properties have attracted increasing interest owing to their potential applications in *e.g.* mechanosensors, security inks, and wearable technologies.[1] Most notably, current research on MCL has been focused exclusively on single-component solid-state emissive dyes,[2–4] and little is known about the mechanoresponsive behavior of two-component dyes.[5] In all previously reported two-component MCL systems, two kinds of organic dyes with good mechanoresponsive properties have been mixed in order to achieve tricolor MCL, which is difficult to realize using single-component dyes.[6] As organic dyes with good MCL properties are relatively rare, it would be desirable if poor MCL properties of organic dyes could be improved upon mixing with another organic fluorophore that exhibit no MCL properties. However, such systems have not yet been established. In addition, the biggest challenges of achieving such multicolor MCL lie in the mechanism of typical MCL dyes. The emission-color change of a single-component MCL dye between two colors typically arises from a transition of the molecular arrangement from an ordered crystalline state to a disordered amorphous state.[2,4] In some cases, the crystalline state alters the degree of its crystallinity or changes to another crystalline state within a polymorphic relationship (Fig. 1a).[3] Polymorphism is a well-known phenomenon for organic crystals and the MCL properties of polymorphic crystals are well documented.[7] In contrast, polyamorphism of organic compounds has only recently been investigated in the field of pharmaceuticals.[8] The difference of emission properties between polyamorphic states has been overlooked so far, although the emission-color change based on polyamorphism should hold the promise of realizing multicolor MCL. Herein, we report that a mixture of two organic dyes with poor MCL and no MCL properties, respectively, exhibits MCL between three colors with a large shift ($\Delta\lambda_{em} \leq 135$ nm) of the emission maximum. We propose that the emission-color change between three colors should be attributed to a transition of a fraction of the MCL dye between one crystalline and two amorphous phases (Fig. 1b).

Results and discussion

For the purpose of developing a new organic dye with MCL properties, we designed 5,5′-dihexyl-3,3′-di(pyren-1-yl)-2,2′-bithiophene (**1**), which is expected to form a mechanical-

Department of Advanced Materials Chemistry, Graduate School of Engineering, Yokohama National University, 79-5 Tokiwadai, Hodogaya-ku, Yokohama 240-8501, Japan. E-mail: suguru-ito@ynu.ac.jp

† Electronic supplementary information (ESI) available: Experimental details, spectral data, DSC thermograms, and fluorescence lifetime decays. See DOI: 10.1039/c8ce01698d

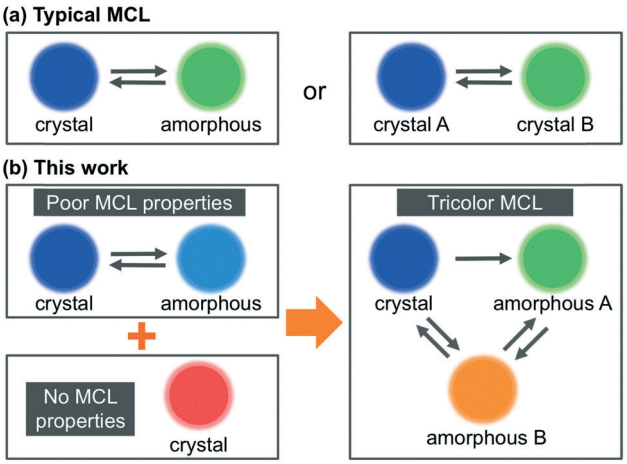

Fig. 1 Schematic illustration for the MCL behavior of organic dyes. (a) Typical MCL: MCL between crystalline and amorphous states, or between two crystalline states (A and B). (b) This work: a two-component dye with tricolor MCL properties by mixing two organic dyes with poor MCL and no MCL properties, respectively.

stimuli-responsive intramolecular stacking between the two pyrenyl rings. Dipyrenylbithiophene **1** was synthesized *via* a Suzuki–Miyaura coupling of pyrene-1-boronic acid with previously reported 3,3′-dibromo-5,5′-dihexyl-2,2′-bithiophene **2** (Fig. 2a).[9] In the presence of 20 mol% of $Pd(PPh_3)_4$, a mixture of dibromide **2** with pyrene-1-boronic acid in 1,4-dioxane/aqueous K_2CO_3 (2 M) was stirred for 12 h at 95 °C to give **1** in 41% yield as a pale-yellow crystalline powder (**B-C**; bithiophene-crystal) after reprecipitation from ethyl acetate. Although the preparation of single crystals suitable for X-ray diffraction analysis was unsuccessful, a ^{1}H NMR analysis of **1** in $CDCl_3$ suggested the existence of intramolecular stacking between the two pyrenyl groups of **1**.[10] **B-C** exhibited a blue fluorescence with a maximum wavelength (λ_{em}) at 488 nm. Upon grinding **B-C** with a spatula, the resulting **B-G** (bithiophene-ground) phase exhibited a bathochromically shifted solid-state emission maximum at 501 nm ($\Delta\lambda_{em}$ = 13 nm).

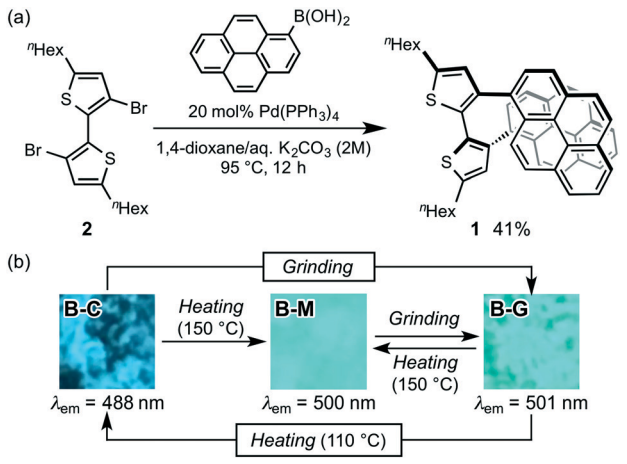

Fig. 2 (a) Synthesis and (b) MCL of dipyrenylbithiophene **1**.

The original blue emission could be recovered upon heating the ground sample in a thermostatic oven to 110 °C (Fig. 2b). In addition, molten amorphous **1** (**B-M**; bithiophene-molten), prepared by heating **B-C** or **B-G** to 150 °C and subsequent cooling to room temperature, exhibited a blue-green emission (λ_{em} = 500 nm). This emission spectrum is almost identical to that of **B-G** prepared by grinding **B-C** or **B-M** (Fig. 2b and Fig. S1†). Powder X-ray diffraction (PXRD) analyses of these samples revealed that the diffraction peaks of crystalline **B-C** disappeared for **B-M** and **B-G** (Fig. S2†). Therefore, the MCL of **1** between **B-C** and **B-G** should be attributed to a typical crystalline-to-amorphous transition. However, the shift of the emission maxima is only 13 nm. This is probably due to the fact that the conformational change of the molecule is, contrary to our initial expectations, relatively small between the crystalline and amorphous states. We speculated that in the presence of another fluorophore an on–off switching of energy transfer from **1** to another fluorophore could be triggered by the transition of **1** from the crystalline to the amorphous states, leading to a significant shift in the solid-state emission maxima upon grinding.

For that purpose, *N*,*N*′-dimethylquinacridone (**DMQA**, Fig. 3a) was selected as the dye to be mixed with **1**, since the red dye **DMQA** exhibits an absorption band around 500 nm in the solid state, which is in the same region as the maximum emission wavelength of **B-G** (Fig. S3†). A 1 : 1 molar mixture of **1** and **DMQA** on a glass plate was molten on a hot plate at 150 °C and then cooled to room temperature. The

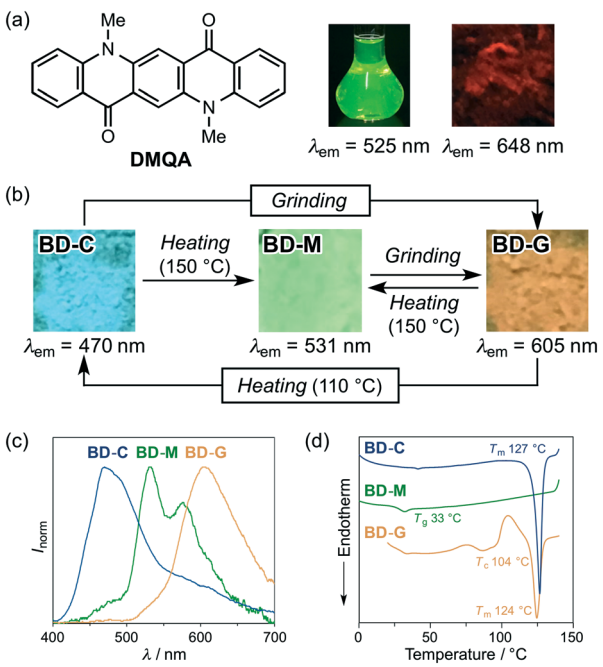

Fig. 3 (a) Structural formula of **DMQA** and photographic images for its emission in toluene and in the solid state. (b) Tricolor MCL of a two-component dye prepared from **1** and **DMQA**. (c) Normalized fluorescence spectra of **BD-C**, **BD-M**, and **BD-G**. (d) DSC thermograms for **BD-C**, **BD-M**, and **BD-G**. T_m, T_g, and T_c values are noted near the corresponding peaks and steps.

mixed dye **BD-M** (bithiophene/**DMQA**-molten) exhibited a green emission with two emission maxima at 531 nm (stronger) and 576 nm (weaker) (Fig. 3b and c), which are different from the solid-state emission maxima of **1** [λ_{em} = 488 nm (crystalline) and 500–501 nm (amorphous); Fig. 2] and **DMQA** (λ_{em} = 648 nm; Fig. 3a). When **BD-M** was scratched and ground with a spatula, a bathochromically shifted orange emission (λ_{em} = 605 nm) was observed from the resulting **BD-G** (bithiophene/**DMQA**-ground) state. Upon heating to 150 °C, **BD-G** was retro-converted into the green-emissive **BD-M**, *i.e.*, this two-component dye exhibits MCL. The transformation between **BD-M** and **BD-G** is fully reversible and could be repeated more than five times (Fig. S4a†). Differential scanning calorimetry (DSC) measurements of **BD-M** and **BD-G** revealed a difference in thermal behavior (Fig. 3d). In the DSC thermogram of **BD-M**, a glass-transition temperature (T_g) was observed at 33 °C. For **BD-G**, on the other hand, an exothermic cold-crystallization transition temperature (T_c) was observed at 104 °C, followed by an endothermic peak that corresponds to the melting point (T_m) at 124 °C.

As the DSC analysis of **BD-G** showed a cold-crystallization peak at 104 °C, **BD-G** was heated in an oven to 110 °C. Interestingly, the emission color of the sample changed to blue (λ_{em} = 470 nm) after heating. This blue-emissive **BD-C** (bithiophene/**DMQA**-crystallized) state could be transformed into the orange-emissive **BD-G** upon grinding. In other words, the two-component dye exhibited MCL between **BD-C** and **BD-G** together with a large shift of the maximum emission wavelength ($\Delta\lambda_{em}$ = 135 nm) (Fig. 3b and c). This transformation is also fully reversible and could be repeated more than five times (Fig. S4b†). The DSC thermogram of **BD-C** showed T_m = 127 °C (Fig. 3d) and when **BD-C** was heated to 150 °C, the two-component dye returned to the initial **BD-M** state (Fig. 3b).[11]

Powder X-ray diffraction (PXRD) analyses of **BD-C**, **BD-M**, and **BD-G** provided mechanistic insights into the tricolor MCL of the mixture of **1** and **DMQA**. The PXRD pattern of **BD-C** was in good agreement with a superposition of those of **1** (**B-C**) and **DMQA**, indicating that **1** and **DMQA** exist as independent crystals in **BD-C** (Fig. 4a–c). Therefore, the blue emission of **BD-C** should be attributed to the emission of **1**

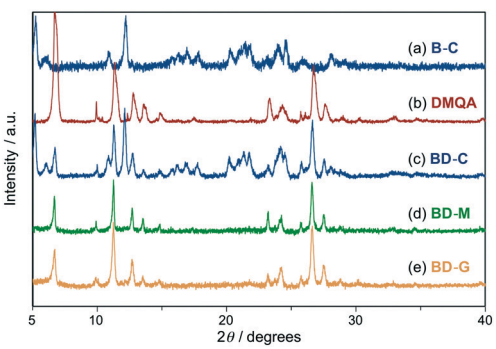

Fig. 4 PXRD patterns for **B-C** (a), **DMQA** (b), **BD-C** (c), **BD-M** (d), and **BD-G** (e).

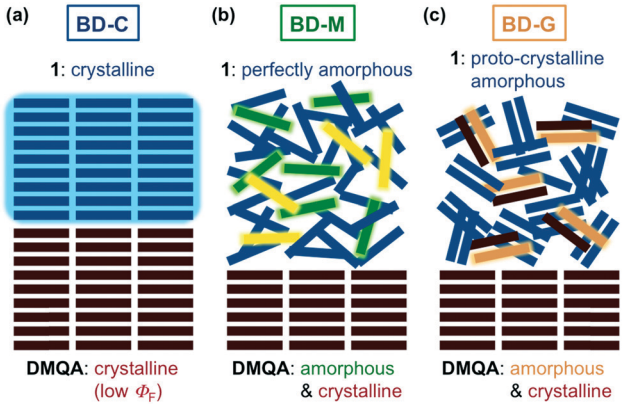

Fig. 5 Schematic illustration for the proposed mechanism of tricolor MCL in the (a) **BD-C**, (b) **BD-M**, and (c) **BD-G** states.

owing to the low fluorescence quantum yield of red-emissive **DMQA** (Fig. 5a; Table 1, Φ_F < 0.01). A slight hypsochromic shift in the maximum emission wavelength of **BD-C** (λ_{em} = 470 nm) compared to **B-C** (λ_{em} = 488 nm) would be explained by the absorption of the emission from **1** into **DMQA**. On the other hand, the observed diffraction pattern for **BD-M** was in good agreement with that of **DMQA** and diffraction peaks attributable to **1** were not observed (Fig. 4d). Similarly, the PXRD analysis of **BD-G** revealed that amorphous **1** and crystalline **DMQA** exist therein (Fig. 4e). Thus, significant differences between the PXRD patterns of **BD-M** and **BD-G** were not observed although their emission colors vary substantially. The fluorescence spectrum of **BD-M** was similar to those of a green-emissive toluene solution of **DMQA** (λ_{em} = 525 nm) and **DMQA**-doped organic light-emitting diodes (λ_{em} = 530–540 nm),[12] although the emission color of **DMQA** is red (λ_{em} = 648 nm) in the solid state (Fig. 3a, Fig. S5†). While the PXRD analysis suggested the existence of crystalline **DMQA** in **BD-M**, some portion of **DMQA** would be dissolved as monomer in the fraction of amorphous **1**, and the green emission of **BD-M** should most likely be rationalized in terms of an emission of dissolved **DMQA** that results from an energy transfer from **1** to dissolved **DMQA** (Fig. 5b). A significantly higher fluorescence quantum yield (Φ_F = 0.016) and a longer area-weighted mean fluorescence lifetime ($\langle\tau_F\rangle$ = 10.6 ns) were observed for **BD-M** compared to red-emissive solid-state **DMQA** (Φ_F < 0.01; $\langle\tau_F\rangle$ = 3.0 ns), supporting the

Table 1 Maximum wavelengths of the solid-state emission (λ_{em}), fluorescence quantum yield (Φ_F), and area-weighted mean fluorescence lifetime ($\langle\tau_F\rangle$) of the two-component dyes (**BD-C**, **BD-M**, and **BD-G**) and **DMQA**

Sample	λ_{em}[a] [nm]	Φ_F[b]	$\langle\tau_F\rangle$[c] [ns]
BD-C	470	0.011	5.1
BD-M	531	0.016	10.6
BD-G	595	0.027	10.5
DMQA	648	<0.01	3.0

[a] Excited by UV light (365 nm). [b] Measured using an integrating sphere. [c] $\langle\tau_F\rangle = \sum(A_n\cdot\tau_n^2)/\sum(A_n\cdot\tau_n)$; *cf.* Fig. S10 and Table S1.

energy transfer from **1** to dissolved **DMQA**. As the **BD-G** state also exhibits a higher fluorescence quantum yield (Φ_F = 0.027) and longer area-weighted mean fluorescence lifetime ($<\tau_F>$ = 10.5 ns) than red-emissive **DMQA**, the energy transfer from amorphous **1** to dissolved **DMQA** should also occur in **BD-G** (Table 1). It should also be noted that both a primary emission peak (λ_{em} = 531 nm) and a shoulder peak (λ_{em} = 576 nm) of **BD-M** should be assigned as monomer emissions of **DMQA** because the same emission peaks were observed from monomer **DMQA** in solutions (Fig. S5†). In addition, upon changing the molar ratio of **1** and **DMQA** from 1 : 1 to 4 : 1, a hypsochromic shift of the emission maximum and a increase of the shoulder peak around 530–540 nm were observed for **BD-G** (Fig. S6†). This hypsochromic shift caused by increasing the ratio of less-polar **1** should be explained by the solvatofluorochromic property of **DMQA** (Fig. S5†).[13] Accordingly, the emission of **BD-G** should be assignable to the bathochromically-shifted monomer emission of **DMQA** (Fig. 3c and Fig. 5b and c).

In the solid-state ^{13}C NMR spectra of **BD-C**, **BD-M**, and **BD-G**, a considerable difference of the chemical shift values was observed between **BD-C**, which includes crystalline **1**, and **BD-M** and **BD-G**, both of which include amorphous **1** (Fig. S8†). More importantly, a significant difference was observed in the alkyl region of the solid-state ^{13}C NMR spectra of **BD-M** and **BD-G**, *i.e.*, the signals of the hexyl groups of **1** in **BD-M** (δ = 31.38, 23.13, 14.66 ppm) were upfield shifted relative to those of **BD-G** (δ = 31.93, 23.58, 14.98 ppm). This result suggests that the hexyl groups of **1** in **BD-M** more efficiently surround **DMQA** and are thus exposed to a stronger shielding effect from **DMQA** than those in **BD-G**.

The differences observed in the DSC analyses and ^{13}C NMR spectra suggest that the fraction of bithiophene **1** should exist in different amorphous states in **BD-M** and **BD-G**. Judging from the thermal behavior and the PXRD pattern of bithiophene **1** in the absence of **DMQA** (Fig. 2, Fig. S2 and S9†), the **B-M** and **B-G** states should correspond to the fraction of **1** in **BD-M** and **BD-G** states, respectively. However, virtually identical emission spectra were observed for **B-M** and **B-G**. In other words, upon addition of **DMQA**, the two amorphous states of **1** can be visualized by the difference in the emission color.

The two amorphous states of **1** are considered to be a perfectly amorphous and a proto-crystalline amorphous state, respectively.[8,14] The perfectly amorphous state refers to a completely disordered state without short- and long-range order, whereas the proto-crystalline amorphous state refers to a partially ordered state that exhibits some short-range order, albeit in the absence of crystallinity. The concept of perfectly and proto-crystalline amorphous states provides a reasonable explanation for the difference in the thermal behavior and emission color between **BD-M** and **BD-G**. In the molten sample **BD-M**, **1** should exist in the perfectly amorphous state as the molecular alignment of **1** would be completely disordered upon melting (Fig. 5b). It has been reported that some molten samples of organic MCL dyes may crystallize on heating and others may not.[4a] A relatively high fluidity of the supercooled liquid state of **1** with two hexyl groups would prevent the formation of ordered alignments on heating, which might be one reason for the no crystallization of molten **1** (**BD-M** and **B-M**) on heating. The observed emission color of **DMQA** (green) in **BD-M** should thus be attributed to the perfectly amorphous and highly mobile **1**, which should act like a hydrocarbon solvent to dissolve some portion of **DMQA**. The exposure of **BD-M** to mechanical stimuli would induce short-range alignments of **1**, and the resulting **BD-G** should thus contain proto-crystalline amorphous **1** (Fig. 5c). Meanwhile, the highly-ordered crystalline structure of **1** in **BD-C** should be destroyed to afford **BD-G** which contains proto-crystalline amorphous **1**. The proto-crystallinity of **BD-G** is supported by the facts that **BD-G** exhibits a cold-crystallization process at 104 °C and no diffraction peaks attributable to long-range order. It would be reasonable to explain that the facile crystallization of **BD-G** on heating is due to the presence of some short-range alignments of **1**. The maximum emission wavelength of **BD-G** is longer than that of **BD-M**. This difference could be explained by the fact that the nonpolar-solvent-like effect of proto-crystalline amorphous **1** is weaker than that of perfectly amorphous **1**. As there are partially ordered domains of **1** in the proto-crystalline amorphous state, **DMQA** should be less surrounded by **1**, which is supported by the results of the solid-state ^{13}C NMR analyses (Fig. S8†) and the emission spectra of **BD-G** prepared from different mixing ratios (Fig. S6†). Accordingly, the intermolecular interaction between **DMQA** molecules should be larger in **BD-G** than in **BD-M**, which leads to the bathochromically-shifted fluorescence owing to the solvatofluorochromic nature of **DMQA** (Fig. 5c and S5†).

Conclusions

In summary, a tricolor mechanochromic luminescence (MCL) that exhibits the large shift in the solid-state emission maximum has been realized by mixing dipyrenylbithiophene **1**, which exhibits poor MCL properties, and **DMQA**, which does not exhibit MCL properties. This study thus is, to the best of our knowledge, the first example of significantly improved MCL properties of an organic dye by adding an organic dye without MCL properties. The origin of the tricolor switch should be attributed to the fraction of **1** in this two-component dye. Importantly, the difference between the two amorphous states of **1** that could not be characterized by PXRD analysis has been clearly distinguished as the difference in emission color. The basic concept of this study, *i.e.*, the mixing of mechanochromic and non-mechanochromic fluorophores has advantages in terms of the availability of MCL dyes and the variety of potential combinations of two-component dyes and should thus generate a variety of new MCL systems with unique properties. Eventually, this should lead to the development of new fundamental insights and practical applications of MCL-active dyes. Further studies on

other two-component MCL systems are currently in progress in our laboratory.

Experimental

General

All air-sensitive experiments were carried out under an atmosphere of argon unless otherwise noted. IR spectra were recorded on a Nicolet iS10 FT-IR spectrometer. ^{1}H and ^{13}C NMR spectra were recorded on a Bruker DRX-500 spectrometer (500 MHz for ^{1}H and 126 MHz for ^{13}C) using tetramethylsilane (0 ppm for ^{1}H and 77.00 ppm for ^{13}C) as an internal standard. Solid-state ^{13}C NMR spectra were recorded on a Bruker Avance III 600 MHz spectrometer (151 MHz for ^{13}C) equipped with an E-free probe for 4.0 mm outer diameter rotors. The samples for solid-state ^{13}C CP-MAS (magic angle spinning) NMR measurements were packed into a 4.0 mm o.d. zirconia NMR rotor. ^{13}C CP-MAS NMR experiments were performed at MAS frequency 11.0 kHz and temperature 298 K. Spinal-64 proton high power decoupling[15] of 78 kHz was employed during each ^{13}C acquisition. ^{13}C chemical shifts were externally referenced to the methyl carbon resonance of adamantane at 38.48 ppm (TMS at 0.0 ppm).[16] A miniature fiber-optic spectrometer (FLAME-S-XR1-ES, Ocean Optics) and a handy UV lamp (365 nm, LUV-6, AS ONE) were used for the measurements of mechanochromic luminescence. Fluorescence and diffuse reflectance spectra were measured on a JASCO FP-8300 fluorescence spectrometer. The absolute fluorescence quantum yields were determined using a 100 mm ϕ integrating sphere JASCO ILF-835. Fluorescence lifetime measurements were recorded on a nanosecond visible/near-infrared fluorescence spectrometer (VITA). The curve-fitting analyses of fluorescence lifetime decays were carried out by using Origin 2018 (OriginLab). Powder X-ray diffraction (PXRD) measurements were performed on a Rigaku SmartLab system using CuKα radiation. DSC data were recorded on a Seiko Instruments DSC-6100 equipped with a liquid nitrogen cooling unit (heating rate: 10 °C min^{-1}). Melting points were determined on a Stuart melting point apparatus SMP3 and uncorrected. High-resolution mass spectrum (HRMS) was recorded on a JEOL JMS-700 mass spectrometer (EI). Silica gel 60 N (spherical, neutral, 63–210 μm) was used for column chromatography. LC analyses were done on silica-gel 60 F_{254}-precoated aluminum backed sheets (E. Merck). 3,3′-Dibromo-5,5′-dihexyl-2,2′-bithiophene (2) was synthesized according to the literature procedure.[9] Other reagents were commercially available.

Synthesis of 5,5′-dihexyl-3,3′-di(pyren-1-yl)-2,2′-bithiophene (1). To a stirred solution of 1-bromopyrene (9.37 mmol 2.63 g) in THF (40 mL), a hexane solution of *n*-BuLi (2.6 M, 14.1 mmol, 6.50 mL) was added dropwise through a syringe at −78 °C. To the mixture was added dropwise triisopropyl borate (18.7 mmol, 3.52 g) at −78 °C, and the reaction mixture was gradually warmed to room temperature and stirred for 24 hours. To the reaction mixture was added 2 M aqueous HCl, and the organic layer was separated. The aqueous layer was extracted with ethyl acetate three times, and the combined organic layer was washed with water and brine, and dried over anhydrous Na_2SO_4. After removal of the solvent under reduced pressure, crude pyrene-1-boronic acid was used directly in the next step.

The mixture of pyrene-1-boronic acid and 3,3′-dibromo-5,5′-dihexyl-2,2′-bithiophene (2, 3.65 mmol, 1.8 g) in 1,4-dioxane (50 mL) and 2 M aqueous K_2CO_3 solution (9 mL) was degassed under ultrasonic irradiation. To the mixture was added $Pd(PPh_3)_4$ (0.70 mmol, 813 mg), and the mixture was further degassed under ultrasonic irradiation. After the mixture was stirred at 95 °C for 12 h, water and dichloromethane were added to the mixture. The organic layer was separated and the aqueous layer was extracted with dichloromethane three times. The combined organic layer was washed with water and brine, and dried over anhydrous Na_2SO_4. After removal of the solvent under reduced pressure, crude product was purified with silica-gel column chromatography (hexane/toluene = 8 : 1) followed by washing with hexane, and reprecipitated from ethyl acetate to give 5,5′-dihexyl-3,3′-di(pyren-1-yl)-2,2′-bithiophene (1) in 41% yield (1.1 g) as pale yellow powder.

5,5′-Dihexyl-3,3′-di(pyren-1-yl)-2,2′-bithiophene (1).

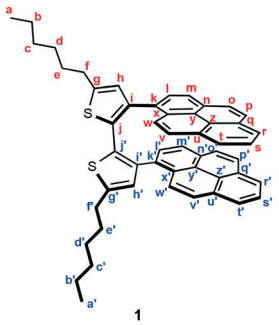

1

41% yield; pale yellow solid; Mp. 125–126 °C; IR (KBr): ν_{max} 3036, 2927, 2825, 1907, 1602, 1585, 1509, 1488, 1465, 1376, 1328, 1243, 1195, 1176, 1150, 1115, 1093, 1074, 961, 949, 930, 889, 839, 823, 792, 751, 717, 683 cm^{-1}; ^{1}H NMR (500 MHz, $CDCl_3$, 283 K): δ (ppm) 8.07 (d, J = 7.6 Hz, 1H, H*r*′), 7.92 (t, J = 7.6 Hz, 1H, H*s*′), 7.81 (d, J = 7.6 Hz, 1H, H*t*′), 7.65 (d, J = 8.3 Hz, 1H, H*m*), 7.64 (d, J = 8.8 Hz, 1H, H*p*′), 7.58 (d, J = 7.3 Hz, 1H, H*r*), 7.54 (t, J = 7.3 Hz, 1H, H*s*), 7.51 (d, J = 8.5 Hz, 1H, H*o*), 7.47 (d, J = 7.3 Hz, 1H, H*t*), 7.45 (d, J = 8.5 Hz, 1H, H*p*), 7.44 (d, J = 8.3 Hz, 1H, H*l*), 7.15 (d, J = 8.8 Hz, 1H, H*o*′), 7.07 (d, J = 7.7 Hz, 1H, H*m*′), 7.04 (d, J = 9.3 Hz, 1H, H*w*′), 7.01 (d, J = 9.3 Hz, 1H, H*v*), 7.00 (d, J = 7.7 Hz, 1H, H*l*′), 6.96 (d, J = 9.3 Hz, 1H, H*w*), 6.89 (d, J = 9.3 Hz, 1H, H*v*′), 6.63 (s, 1H, H*h*), 6.52 (s, 1H, H*h*′), 2.84–2.77 (m, 4H, H*f*, H*f*′), 1.75–1.67 (m, 4H, H*e*, H*e*′), 1.42–1.36 (m, 4H, H*d*, H*d*′), 1.33–1.28 (m, 8H, H*b*, H*b*′, H*c*, H*c*′), 0.92–0.87 (m, 6H, H*a*, H*a*′); ^{13}C NMR (126 MHz, $CDCl_3$, 283 K): δ (ppm) 145.3 (C*g*′), 145.1 (C*g*), 138.9 (C*i*), 137.5 (C*i*′), 131.53 (C*k*′), 131.52 (C*k*), 130.9 (C*q*′), 130.5 (C*u*′), 130.2 (C*j*′), 130.05 (C*j*), 130.01 (C*q*), 129.73 (C*n*), 129.67 (C*u*), 129.3 (C*n*′), 129.0 (C*h*′), 128.4 (C*h*), 127.8 (C*x*), 127.4 (C*l*), 127.2 (C*x*′), 126.8 (C*l*′), 126.45 (C*o*′), 126.44 (C*p*′),

126.3 (C*o*), 126.2 (C*p*), 125.7 (C*v*′), 125.6 (C*v*), 125.2 (C*s*′), 124.8 (C*s*), 124.38 (C*w*′, C*t*′), 124.35 (C*m*), 124.22 (C*z*′), 124.17 (C*r*′, C*r*), 124.1 (C*y*′), 123.8 (C*t*), 123.6 (C*w*), 123.5 (C*y*), 123.4 (C*m*′), 123.1 (C*z*), 31.5 (C*c*′, C*c*), 31.4 (C*e*), 31.3 (C*e*′), 30.2 (C*f*), 30.1 (C*f*′), 28.8 (C*d*), 28.7 (C*d*′), 22.6 (C*b*′, C*b*), 14.2 (C*a*′, C*a*); HRMS-EI (*m*/*z*): $[M]^+$ calcd for $C_{52}H_{46}S_2$, 734.3041; found, 734.3029.

Conflicts of interest

There are no conflicts to declare.

Acknowledgements

This work was partly supported by JSPS KAKENHI Grant Number 18H04508 in Grant-in-Aid for Scientific Research on Innovative Areas "Soft Crystals: Area No. 2903", by the Tonen General Research Foundation, and by the CASIO Science Promotion Foundation. The authors are grateful to Drs. Hiroyuki Matsuzaki and Yusuke Okabayashi for the measurement of the fluorescence lifetime values (National Metrology Institute of Japan, National Institute of Advanced Industrial Science and Technology). The authors also thank Ms. Masayo Ishikawa (Suzukakedai Materials Analysis Division, Technical Department, Tokyo Institute of Technology) for EI-HRMS analyses.

Notes and references

1 For recent reviews, see: (*a*) Y. Sagara, S. Yamane, M. Mitani, C. Weder and T. Kato, *Adv. Mater.*, 2016, **28**, 1073; (*b*) Z. Ma, Z. Wang, M. Teng, Z. Xu and X. Jia, *ChemPhysChem*, 2015, **16**, 1811; For seminal examples on MCL dyes, see: (*c*) Y. Sagara, T. Mutai, I. Yoshikawa and K. Araki, *J. Am. Chem. Soc.*, 2007, **129**, 1520; (*d*) J. Kunzelman, M. Kinami, B. R. Crenshaw, J. D. Protasiewicz and C. Weder, *Adv. Mater.*, 2008, **20**, 119; (*e*) H. Ito, T. Saito, N. Oshima, N. Kitamura, S. Ishizaka, Y. Hinatsu, M. Wakeshima, M. Kato, K. Tsuge and M. Sawamura, *J. Am. Chem. Soc.*, 2008, **130**, 10044; (*f*) T. Abe, T. Itakura, N. Ikeda and K. Shinozaki, *Dalton Trans.*, 2009, 711; (*g*) Y. Ooyama, Y. Kagawa, H. Fukuoka, G. Ito and Y. Harima, *Eur. J. Org. Chem.*, 2009, 5321; (*h*) G. Zhang, J. Lu, M. Sabat and C. L. Fraser, *J. Am. Chem. Soc.*, 2010, **132**, 2160; (*i*) S. Perruchas, X. F. L. Goff, S. Maron, I. Maurin, F. Guillen, A. Garcia, T. Gacoin and J.-P. Boilot, *J. Am. Chem. Soc.*, 2010, **132**, 10967; (*j*) X. Zhang, Z. Chi, H. Li, B. Xu, X. Li, W. Zhou, S. Liu, Y. Zhang and J. Xu, *Chem. – Asian J.*, 2011, **6**, 808; (*k*) X. Zhang, Z. Chi, J. Zhang, H. Li, B. Xu, X. Li, S. Liu, Y. Zhang and J. Xu, *J. Phys. Chem. B*, 2011, **115**, 7606; (*l*) S.-J. Yoon and S. Y. Park, *J. Mater. Chem.*, 2011, **21**, 8338; (*m*) Y. Dong, B. Xu, J. Zhang, X. Tan, L. Wang, J. Chen, H. Lv, S. Wen, B. Li, L. Ye, B. Zou and W. Tian, *Angew. Chem., Int. Ed.*, 2012, **51**, 10782; (*n*) K. Nagura, S. Saito, H. Yusa, H. Yamawaki, H. Fujihisa, H. Sato, Y. Shimoikeda and S. Yamaguchi, *J. Am. Chem. Soc.*, 2013, **135**, 10322; (*o*) M. Krikorian, S. Liu and T. M. Swager, *J. Am. Chem. Soc.*, 2014, **136**, 2952.

2 For recent examples of single-component dyes that exhibit MCL based on crystal-to-amorphous transitions, see: (*a*) S. A. Sharber, K.-C. Shih, A. Mann, F. Frausto, T. E. Haas, M.-P. Nieh and S. W. Thomas, *Chem. Sci.*, 2018, **9**, 5415; (*b*) B. Li, K. Seth, B. Niu, L. Pan, H. Yang and H. Ge, *Angew. Chem., Int. Ed.*, 2018, **57**, 3401; (*c*) D. T. Walters, R. B. Aghakhanpour, X. B. Powers, K. B. Ghiassi, M. M. Olmstead and A. L. Balch, *J. Am. Chem. Soc.*, 2018, **140**, 7533; (*d*) L. Wilbraham, M. Louis, D. Alberga, A. Brosseau, R. Guillot, F. Ito, F. Labat, R. Métivier, C. Allain and I. Ciofini, *Adv. Mater.*, 2018, **30**, 1800817; (*e*) Y. Takeda, T. Kaihara, M. Okazaki, H. Higginbotham, P. Data, N. Tohnai and S. Minakata, *Chem. Commun.*, 2018, **54**, 6847; (*f*) T. Seki, K. Ida and H. Ito, *Mater. Chem. Front.*, 2018, **2**, 1195; (*g*) H. Mori, K. Nishino, K. Wada, Y. Morisaki, K. Tanaka and Y. Chujo, *Mater. Chem. Front.*, 2018, **2**, 573; (*h*) B. Xu, H. Wu, J. Chen, Z. Yang, Z. Yang, Y.-C. Wu, Y. Zhang, C. Jin, P.-Y. Lu, Z. Chi, S. Liu, J. Xu and M. Aldred, *Chem. Sci.*, 2017, **8**, 1909; (*i*) T. Seki, K. Kobayashi and H. Ito, *Chem. Commun.*, 2017, **53**, 6700; (*j*) Y. Jiang, G. Li, W. Che, Y. Liu, B. Xu, G. Shan, D. Zhu, Z. Su and M. R. Bryce, *Chem. Commun.*, 2017, **53**, 3022; (*k*) B. Y.-W. Wong, H.-L. Wong, Y.-C. Wong, V. K.-M. Au, M.-Y. Chan and V. W.-W. Yam, *Chem. Sci.*, 2017, **8**, 6936; (*l*) F. Wang, C. A. DeRosa, M. L. Daly, D. Song, M. Sabat and C. L. Fraser, *Mater. Chem. Front.*, 2017, **1**, 1866; (*m*) M. Okazaki, Y. Takeda, P. Data, P. Pander, H. Higginbotham, A. P. Monkman and S. Minakata, *Chem. Sci.*, 2017, **8**, 2677.

3 For recent examples of single-component dyes that exhibit MCL between different crystalline states, see: (*a*) M. Jin, T. Sumitani, H. Sato, T. Seki and H. Ito, *J. Am. Chem. Soc.*, 2018, **140**, 2875; (*b*) K. K. Neena, P. Sudhakar, K. Dipak and P. Thilagar, *Chem. Commun.*, 2017, **53**, 3641.

4 We have previously reported several single-component organic dyes with MCL properties: (*a*) S. Ito, T. Taguchi, T. Yamada, T. Ubukata, Y. Yamaguchi and M. Asami, *RSC Adv.*, 2017, **7**, 16953; (*b*) S. Ito, T. Yamada and M. Asami, *ChemPlusChem*, 2016, **81**, 1272; (*c*) S. Ito, T. Yamada, T. Taguchi, Y. Yamaguchi and M. Asami, *Chem. – Asian J.*, 2016, **11**, 1963.

5 (*a*) Z. Ma, Y. Ji, Z. Wang, G. Kuang and X. Jia, *J. Mater. Chem. C*, 2016, **4**, 10914; (*b*) H.-J. Kim, D. R. Whang, J. Gierschner, C. H. Lee and S. Y. Park, *Angew. Chem., Int. Ed.*, 2015, **54**, 4330.

6 Only few single-component dyes exhibit tricolor MCL. For examples, see: (*a*) X. Wu, J. Guo, Y. Cao, J. Zhao, W. Jia, Y. Chen and D. Jia, *Chem. Sci.*, 2018, **9**, 5270; (*b*) W. Yang, C. Liu, S. Lu, J. Du, Q. Gao, R. Zhang, Y. Liu and C. Yang, *J. Mater. Chem. C*, 2018, **6**, 290; (*c*) Z. Ma, Z. Wang, X. Meng, Z. Ma, Z. Xu, Y. Ma and X. Jia, *Angew. Chem., Int. Ed.*, 2016, **55**, 519; (*d*) Y. Sagara and T. Kato, *Angew. Chem., Int. Ed.*, 2011, **50**, 9128, See also ref. 2*m* and 4*b*.

7 For a review, see: (*a*) R. Tan, S. Wang, H. Lan and S. Xiao, *Curr. Org. Chem.*, 2017, **21**, 236; For recent examples, see: (*b*) C. Ge, J. Liu, X. Ye, Q. Han, L. Zhang, S. Cui, Q. Guo, G. Liu, Y. Liu and X. Tao, *J. Phys. Chem. C*, 2018, **122**, 15744; (*c*)

P. S. Hariharan, G. Parthasarathy, A. Kundu, S. Karthikeyan, Y. Sagara, D. Moon and S. P. Anthony, *Cryst. Growth Des.*, 2018, **18**, 3971; (*d*) C. Arivazhagan, P. Malakar, R. Jagan, E. Prasad and S. Ghosh, *CrystEngComm*, 2018, **20**, 3162; (*e*) H. Zhu, S. Weng, H. Zhang, H. Yu, L. Kong, Y. Zhong, Y. Tian and J. Yang, *CrystEngComm*, 2018, **20**, 2772.

8 (*a*) G. Zografi and A. Newman, *J. Pharm. Sci.*, 2017, **106**, 5; (*b*) Y. N. Thi, K. Rademann and F. Emmerling, *CrystEngComm*, 2015, **17**, 9029.

9 X. Guo, S. Wang, V. Enkelmann, M. Baumgarten and K. Müllen, *Org. Lett.*, 2011, **13**, 6062.

10 Dipyrenylbithiophene **1** should form intramolecular stacks of pyrene groups as shown in Fig. 2a, since the ^{1}H NMR signals of the two non-equivalent pyrenyl groups in **1** are upfield shifted relative to those of pyrenyl groups of reported pyrenylthiophene derivatives. For ^{1}H NMR spectra of pyrenylthiophene derivatives, see: (*a*) M. Ashizawa, K. Yamada, A. Fukaya, R. Kato, K. Hara and J. Takeya, *Chem. Mater.*, 2008, **20**, 4883; (*b*) Y. Aso, T. Okai, Y. Kawaguchi and T. Otsubo, *Chem. Lett.*, 2001, **30**, 420.

11 As the melting point of **DMQA** (286 °C, decomp.) is above 150 °C, only the fraction of bithiophene **1** should be liquefied upon heating to 150 °C.

12 (*a*) H. Liu, F. Yan, W. Li, B. Chu, W. Su, Z. Su, J. Wang, Z. Hu and Z. Zhang, *Appl. Phys. Lett.*, 2010, **96**, 083301; (*b*) Z. Su, W. Li, B. Chu and S. Wu, *Thin Solid Films*, 2011, **519**, 2540.

13 Another possible explanation for the bathochromically-shifted emission of **BD-G** is the partial quenching of the emission by the absorption of **DMQA**. However, this explanation would be less probable because there is only a slight difference between the solid-state absorption spectra of **BD-M** and **BD-G** (Fig. S7†).

14 D. Q. M. Craig, V. L. Kett, J. R. Murphy and D. M. Price, *Pharm. Res.*, 2001, **18**, 1081.

15 B. M. Fung, A. K. Khitrin and K. Emolaev, *J. Magn. Reson.*, 2000, **142**, 97.

16 R. K. Harris, E. D. Becker, S. M. Cabral de Menezes, P. Granger, R. E. Hoffman and K. W. Zilm, *Pure Appl. Chem.*, 2008, **80**, 59.